Corrosion Protection by Novel Conversion Coatings on Structural Al 6061

Article *in* Applied Science and Engineering Progress · January 2023

DOI: 10.14416/j.asep.2022.03.005

7 authors, including:

Makanjuola Oki
Landmark University
61 PUBLICATIONS **413** CITATIONS
SEE PROFILE

Adeolu Adesoji Adediran
Landmark University
203 PUBLICATIONS **1,047** CITATIONS
SEE PROFILE

Ikechukwu K Anyim
Landmark University
3 PUBLICATIONS **2** CITATIONS
SEE PROFILE

Charles Onokohwomo
Landmark University
1 PUBLICATION **0** CITATIONS
SEE PROFILE

Research Article

Corrosion Protection by Novel Conversion Coatings on Structural Al 6061

Makanjuola Oki*, Adeolu Adesoji Adediran*, Anyim Ikechukwu, Charles O. Onokohwomo and Chuka Bosa
Department of Mechanical Engineering, College of Engineering, Landmark University, Omu-Aran, Kwara State, Nigeria

Sarah A. Akintola
Department of Petroleum Engineering University of Ibadan, Ibadan, Nigeria

Olanrewaju Seun Adesina
Department of Mechanical Engineering, College of Engineering, Landmark University, Omu-Aran, Kwara State, Nigeria
Department of Mechatronics Engineering, Bowen University, Nigeria

* Corresponding author. E-mail: makanjuola.oki@lmu.edu.ng, adediran.adeolu@lmu.edu.ng
DOI: 10.14416/j.asep.2022.03.005
Received: 24 August 2021; Revised: 13 September 2021; Accepted: 3 February 2022; Published online: 21 March 2022

Abstract
Chromate conversion coatings have witnessed limited acceptability in recent times. The coatings contain Cr (VI) species that have been classified as environmental hazards and injurious to human health. Thus, the use of environment-friendly and non-carcinogenic novel inorganic-inorganic hybrid conversion coatings are being explored. Vanadate (VCC), hybrid Vanadate/Molybdate (HCC) conversion coatings on Al6061 have been classified in terms of corrosion and adhesion performance with reference to the untreated alloy. Natural exposure tests in the atmosphere and stagnant near-neutral 3.5% sodium chloride solution, as well as potentio-dynamic polarization measurements showed that the corrosion rate for HCC is lower for Vanadate, which in turn outclassed the 'bare' alloy. However, clusters of passive incipient pits were revealed on the former after 120 h of exposure in stagnant chloride solution. Both conversion coatings outperformed the untreated aluminium alloy after atmospheric corrosion and adhesion tests.

Keywords: Conversion coatings, Molybdate, Vanadate, Chromate, Aluminium alloy

1 Introduction

Several protocols of chromate conversion coatings placed various limitations on the use of chromates in industries including aluminium finishing and construction outfits [1], [2]. Al6061 is mostly employed for architectural purposes, which are not limited to roofing but for frames, sliding, and partitioning within buildings. These aluminium alloys are usually coated with chromates for long-term corrosion prevention and paint adhesion purposes. Thus, apart from interactions of workers with chromates during finishing and fabrication of aluminium alloys, there are exist levels of residual chromates in alloy products.

Although anodized aluminium alloys from environment-friendly solutions may exhibit superior corrosion protection than conversion coated alternatives, however, conversion coatings with good qualities are usually applied at low costs and easily by simple immersion or swabbing/touch procedures [3]. Hence, conversion coatings can be employed in touch protection repairs of cut edges during the fabrication of architectural parts. It is generally known that chromates have satisfied these conditions as well as

superior self-repair characteristics [4], [5]. Thus, any conversion coating process, which will replace the chromate [6], [7] must satisfy these pre-conditions as well as be environment friendly [8] and non-carcinogenic [9]. Various conversion coating processes with the use of permanganate [10], manganate [11], Zirconium [12] Molybdenum [11] have been reported in the literature. The majority of these, although with lower toxicity than the chromates, have not displayed corrosion protection superiority over the chromate nor their paint adhesion capacities. Those with superior corrosion protection are based on Zr/Cr III [13] and a novel hybrid conversion coating derived from water extracts of Hibiscus sabdariffa calyx in conjunction with ammonium molybdate [1]. The Zr/Cr III is the most popular in the current usage and was thought to be free of chromate [14]. Its Cr III content is readily acceptable within the context of carcinogenicity and environmental hazard.

However, recent findings [15], [16] have indicated that the chromium in +3 oxidation state can readily be converted to the +6 oxidation state through oxidation by H_2O_2, which was produced by an oxygen reduction reaction [15]. These finding put a big question mark on the continuous use of the conversion coating. Thus, more vigorous efforts are severally directed towards finding a lasting replacement for chromate conversion coatings without any forms of chromium compounds in the coating bath.

Although other eco-friendly alternatives are being researched, the current effort compares the corrosion protection capabilities of the novel inorganic-inorganic conversion coating. These have been developed from environment-friendly coating baths and examined in natural atmospheric exposure tests and 3.5% near-neutral sodium chloride solution.

2 Experimental Techniques

2.1 *Materials*

Aluminium 6061, with nominal composition of 96.85% Al, 0.9% Mg, 0.7% Si, 0.6% Fe, 0.3% Cu, 0.25% Cr, 0.20% Zn, 0.10% Ti, 0.05% Mn, and 0.05% others was made out into spade-like electrodes, etched in 10% NaOH, rinsed in water, de-smutted in 50% w/w HNO_3, rinsed in water, dried in air for 25 min and stored in a desiccator. Conversion coating solutions were prepared in 1 liter of water, containing (a) HCC; Mix, MCC: VCC in ratio 1:1, where MCC was made up as follows, 4 g/L ammonium molybdate and 1 g/L NaF and (b) 4 g/L metavanadate and 2 g/L NaF. Then, the pH values of all conversion coating solutions were adjusted to between pH 3.5 to 4 with either NaOH or HNO_3. All chemicals are laboratory grade purchased from BDH Chemicals, UK.

2.2 *Gravimetric analysis*

The cleaned electrodes were immersed separately in the conversion coating baths for various times ranging from 30 s to 10 min with weight measurements taken before and after immersion in the respective coating solutions. After each immersion period, they were rinsed in running water and dried overnight at room temperature.

2.3 *Electrochemical analysis*

For potentiodynamic measurements, untreated Al6061 and specimens treated for 3 min each in the coating baths were mounted in a resin such that, as working electrodes, they have an exposed area of 1.13 cm^2 each. With the use of Digi-Ivy 2300 potentiostat and a three-electrode cell comprising of platinum as a counter electrode, silver/silver chloride (Ag/AgCl) as reference electrode, while the various specimens served severally as working electrodes. Measurements were carried out from –1.5 V to +1.5 V at a scan rate 0.0016 V/s according to ASTM G102-89 (2015). The measurements were performed at 24, 72, and 120 h of immersion of the various specimens in 150 mL of 3.5% NaCl solution. The corrosion current density, I_{corr}, and the corrosion potential, E_{corr} for the conversion coated specimens and Al 6061 were obtained from the Tafel plots of log current versus potential installed along with the Digi- Ivy 2300 potentiostat.

2.4 *Natural atmospheric NaCl solution exposure tests*

The specimens exposed to the natural environment in the Northcentral region of Nigeria and those exposed to stagnant, near neutral, 3.5% NaCl were treated thus: (a) Conversion coated for 3 min in the respective coating solutions; (b) treated as in (a) but over-coated with a thin layer of nitrocellulose lacquer; (c) uncoated

aluminium and (d) treated as (c) with a thin overcoat of lacquer. Application of the lacquer was performed by pouring the clear lacquer into a 20 mL beaker and individual specimens were immersed as vertical as possible for 25 s. The specimens were withdrawn, drained, and dried as withdrawn. The dried lacquer was 6 µm in thickness as obtained by using a Fischer's instrument Pemascope. All the specimens were cross-scratched, exposed in triplicates, and monitored with naked eyes and photography

3 Results and Discussion

3.1.1 Coating development

The growth pattern for the coatings appears similar, albeit, from initial 0 g in weight at 0 s immersion time to between 1 and 2.0 × 10^{-3} g weight gain at between 60 to 180 s of treatment time, which the VCC showed a superior growth rate as displayed in Figure 1.

The formations of coatings by immersion in the various coating solutions were further reinforced by several color changes observed during coating development studies. The vanadium conversion coating, which developed over the lustrous shiny grey aluminium alloy surface, displayed multiple colors of purple, yellow, and green after 180 s of treatment, which grew more intense with immersion time. However, the hybrid vanadate/molybdate coating displayed green and yellow over a largely dark purple coating material after 180 s of treatment. This suggests at face value that the formation of vanadium II oxide and/or hydroxide may have predominantly formed the bulk of the coating at this instance of coating development. The darker shade of purple suggests the formation and deposition of molybdate compounds incorporated in the conversion coating as Mo in oxidation states of (iv) and possibly (v), which are known to give iridescent to matt brown conversion coatings on aluminium [17]. Thus, the formation and development of these conversion coatings must have followed the known path of activation of Al by fluoride ions in the coating solution with the release of electrons. Equations (1)–(3) further describe this formation.

$$Al \rightarrow Al^{3+} + 3e^{-} \quad (1)$$

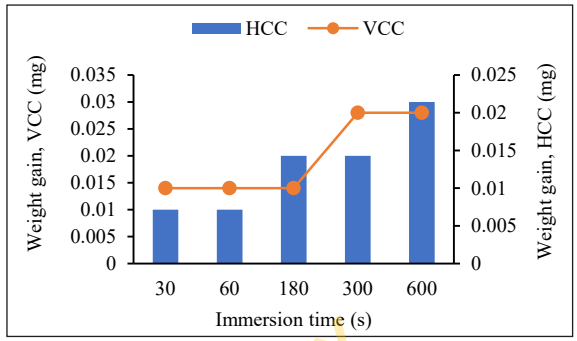

Figure 1: The graphs showing coating weight versus immersion time in VCC and HCC coating baths.

The electrons released in Equation (1) are taken up vanadium (V) in Equation (2) as follows:

$$V^{5+} + 3e^{-} \rightarrow VO \quad (2)$$

To produce hydrated vanadium oxides/or hydroxides in the oxidation state of +2. This is predominantly purple/violet in coloration. Hydrogen evolution is a complimentary cathodic reaction in the acidic bath which made the interfacial pH to rise.

$$3H^{+} + 3e^{-} \rightarrow 3/2H_2 \quad (3)$$

With an increase in pH, vanadium oxide and/or hydroxide is deposited as the conversion coating when it attained the necessary equilibrium conditions. Due to the formation of this initial barrier coating, further oxidation/reduction reactions may proceed through electron tunneling as expounded by other researchers [18], [19]. Hence, the reduction of Vanadium (v) to Vanadium (iv) occurred after picking up an electron to produce blue-colored hydrated oxide variant or hydroxide. The green colored variety of Vanadium in the oxidation state of (III) was also produced on picking up two electrons. Vanadium (v) formed in acidic environments, produced the yellow colored variant observed on the conversion coated specimens. This may have been adsorbed or occluded within the growing multi-colored vanadate conversion coating as displayed in Figures 2(a) and (b) for VCC and HCC. These coatings developed after three minutes of treatment in the respective coating solutions. Three minutes had been adjudged premium treatment time from conversion coating baths [7], [8]. It has been observed that beyond

(a) (b)

Figure 2: Photographs showing deliberately cross-hatched multi-colored conversion coatings developed for 180 s each in (a) VCC and (b) HCC coating baths before exposure tests.

three minutes the coating will become friable as a result of weathering action of the acidic bath [10].

3.1.2 Atmospheric exposure tests

All specimens exposed to the atmosphere for 120 h did not reveal any serious atmospheric corrosion problems. The A16061 without conversion coating displayed only a dull grey appearance, while the specimen over coated with lacquer revealed a yellowish appearance with paint delamination after application of adhesive tape test. The yellowish color may be related to water absorbed by the polymeric material of the lacquer. The color was enhanced by corrosion product due to the transformation of the initial air-formed oxide on the substrate to hydrated aluminium oxide and/or hydroxide during prolonged natural atmospheric exposure.

The VCC and HCC specimens with a top coating of lacquer revealed dull cream coloration due to absorption of moisture by the lacquer. However, over the exposure period, those specimens without top coatings of lacquer had reduced intensities of their colored conversion coating materials. Reduction in color intensities occurred from interactions of the coating material components with moisture and other contaminants in their immediate environments.

3.1.3 Immersion in 3.5% sodium chloride solution

The initial color of the variously treated specimens changed and varied from the initial shiny color of A16061 to dull grey. In addition, corrosion products interspersed with trough-like pits were revealed after 120 h of exposure to the chloride solution. Interestingly

(a) (b)

Figure 3: Photographs of (a) lacquer coated HCC and 'bare' HCC after exposure for 120 h in sodium chloride solution.

the lacquer coated A16061 only displayed carpets of hydrated $Al_2O_3/Al(OH)_3$ underneath the lacquer with some incipient pitting corrosion sites. However, paint delamination was observed after adhesive tape tests. Curiously, the HCC with a top coating of lacquer displayed clusters of passivated pits with a large population density. On the other hand, its counterpart without a covering of lacquer did not portray any form of pitting corrosion other than reduced intensities in the colors of the coating materials as displayed in Figure 3(a) and (b) respectively.

The reducible components in the coating such as vanadium in oxidation states of V, IV, and III protected the substrate through their electrochemical reactions at corrosion susceptible regions. For the specimens carrying a top coating of lacquer, the mobilities of the reducible species were probably impaired, although the incipient pits did not grow bigger (Figure 3) after the first appearance of a few on the second day of exposure. For the VCCs, although physical color changes occurred, pits were not readily visible on both specimens with and without coatings of lacquer. However, trough-like features appeared on the specimens without a coating of lacquer over an exposure period of three days. These are likely flawed regions in the coating where chlorides undermined the coating. The lacquer on its counterpart prevented such chloride ingress, suggesting that composite conversion coating/lacquer gave superior protection. Although HCC and VCC specimens were pre-scratched prior to exposure regimes, paint delamination was not observed on performing adhesive tape tests after 120 h.

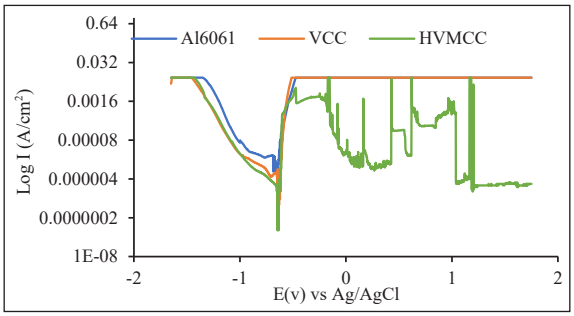

Figure 4: Potentiodynamic polarization curves for Al6061, VCC, and HCC coated specimens in 3.5% NaCl solution.

3.1.4 Potentiodynamic polarization tests

Figure 4 displays the polarization curves for Al6061 and specimens conversion coated in VCC and HCC for 180 s at 24 h of immersion in 3.5% sodium chloride solution while the corresponding electrochemical corrosion data derived therefrom are described in Table 1.

The corrosion rates for HCC and VCC specimens are lower than for untreated aluminium with values of 0.024, 0.092, and 0.549 mm/year respectively. The corresponding corrosion current densities are 2.2×10^{-6}, 8.58×10^{-6}, and 5.09×10^{-5} A/cm^2.

These corrosion rates for the conversion coated specimens are about an order of magnitude lower than for the uncoated Al6061 specimen. This observation is expected since there are barrier coverings of conversion coatings on the treated specimens, which have been reported to be in the order of 1 µm in thickness [20]. The polarization resistance of the specimens and corrosion rates showed large differences, with HCC having a value of about 11.7 kΩ, followed by VCC with 3 kΩ and untreated Al 6061 with the least resistance of about 0.51 kΩ reflecting the trend in their corrosion rates. In case of the Tafel anodic constants, Ba whose values are widely different ranging from 7.1 V/dec

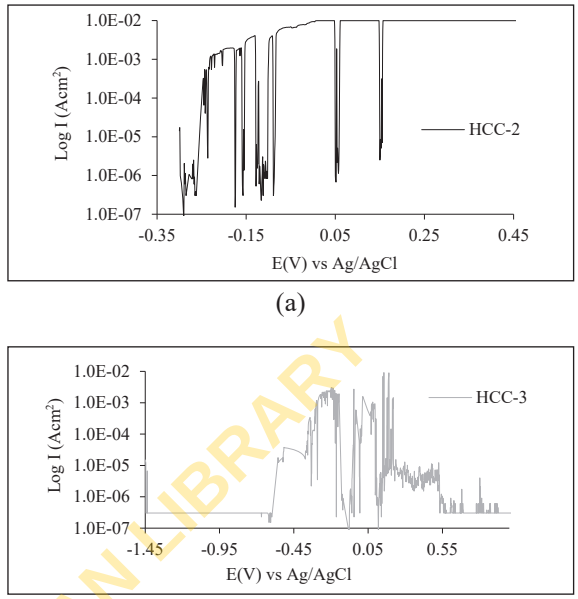

Figure 5: Polarization curves for HCC in NaCl solution at (a) 72 h and (b) 120 h exposure in 3.5% NaCl.

for HCC to 21.6 V/dec for VCC and about 16 V/dec for Al6061 indicated difference of anodic dissolution reaction mechanisms.

However, the anodic polarization for HCC displayed some characteristic features of frequent surges in current density, which may generally be referred to as crack and heal effects of pit initiation and passivation [21], [22] by easily reducible molybdate species in the coating materials [23], [24]. As a time of immersion progressed, the current surges became more erratic as displayed in Figure 5(a) and (b) present are the polarization curves for HCC at 72 and 120 h of immersion in 3.5% NaCl solution. This behavior rendered anodic polarization of the specimens impossible, thus corrosion parameters became indeterminate

The polarization curves for Al6061 and VCC conversion coated specimens at 72 and 120 h of

Table 1: Corrosion parameters derived from Tafel at 24 h of polarization measurement

Specimen	Corrosion Rate (mm/y)	Corrosion Current (A)	Corrosion Current Density (A/cm^2)	Corrosion Potential (V)	Polarization Resistance, R_p (Ω)	Cathodic Potential, B_c V/dec)	Anodic potential, B_a (V/dec)
Al6061	0.549	5.09E-05	5.09E-05	–0.641	504.9	0.818	16.310
VCC	0.092	8.58E-06	8.58E-06	–0.634	2995.0	–0.895	21.590
HCC	0.024	2.20E-06	2.20E-06	–0.636	11690.0	–3.082	7.114

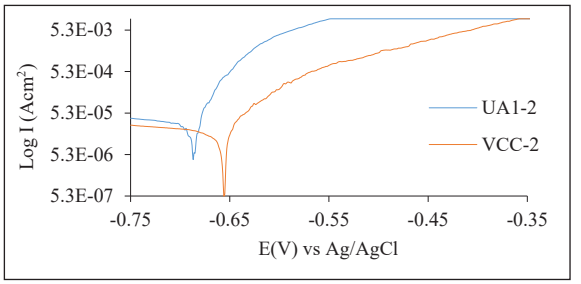

(a)

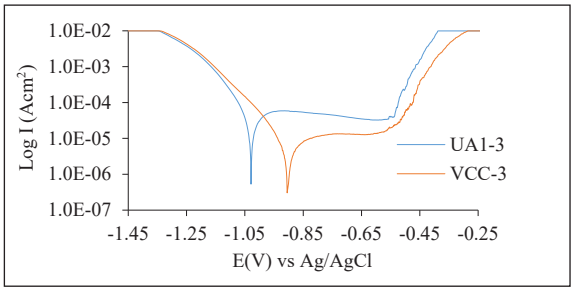

(b)

Figure 6: Polarization curves for Al6061 and VCC coated specimens at (a) 72 h and (b) 120 h in 3.5% NaCl.

exposure to chloride solution are displayed in Figure 6(a) and (b), respectively with the corresponding corrosion data derived from the curves displayed in Tables 2 and 3, respectively.

From Table 2 the corrosion rate for VCC decreased further at 72 h of immersion to 0.076 mm/year with a corresponding increase in polarization resistance to 3.3 kΩ, whereas the rate for Al6061 increased to 0.575 mm/year and lower polarization resistance of 0.48 kΩ. Thus, the conversion coated specimen showed a superior corrosion performance to the untreated Al6061. Interestingly, at 120 h of exposure, the corrosion rate for Al6061 decreased in value to 0.39 mm/year, about 200 folds decrease compared with the rate at 72 h of exposure. This observation may be related to the self-healing/sealing as occasioned by the formation of oxides of Al aided by passivation activities of the chromium content in the alloy [25]. After protracted exposure in the saline environment, Cr ions may have been released appreciably to aid such passivity giving a passive current density of 3.62 × 105A/cm^2

For the VCC, a trend towards reduced corrosion rate was maintained at 120 h of exposure. The value of the corrosion rate reduced further to 0.062 mm/year indicating that the conversion coating is still functional as a barrier to corrosion and the reducible vanadium contents of the coating were still active. From Tables 2 and 3, it may be observed that the values of Tafel constants, Ba, are almost similar indication of closely related anodic reaction mechanisms. At this period of exposure, the corrosion potentials of the two specimens are similar at about –1.0 V. Whereas, for the exposure periods 24 h to 72 h, the corrosion potentials for all the specimens hovered around –0.6 V indicating innate thermodynamic predictability for corrosion activities. At 72 and 120 h of exposure in the chloride solution, the polarization curves for VCC and Al 6061 specimens appeared to be similar [Figure 6(a) and (b)] with similar pitting potentials, Epp, at about –0.55V

Table 2: Tafel data generated from polarization curves during immersion in NaCl for 72 h

Specimen	Corrosion Rate (mm/y)	Corrosion Current (A)	Corrosion Current Density (A/cm^2)	Corrosion Potential (V)	Polarization Resistance, R_p (Ω)	Cathodic Potential, B_c V/dec)	Anodic potential, B_a (V/dec)
Al 6061	0.575	5.34E-05	5.34E-05	–0.656	481.4	–1.722	11.390
VCC-2	0.076	7.03E-06	7.03E-06	–0.687	3248.4	–2.254	12.650
HCC-2	-	-	-	-	-	-	-

Table 3: Tafel data generated from polarization curves during immersion in NaCl for 120 h

Specimen	Corrosion Rate (mm/y)	Corrosion Current (A)	Corrosion Current Density (A/cm^2)	Corrosion Potential (V)	Polarization Resistance, R_p (Ω)	Cathodic Potential, B_c V/dec)	Anodic potential, B_a (V/dec)
Al 6061	0.390	3.62E-05	3.62E-05	–1.029	705.0	–11.220	1.687
VCC	0.062	5.72E-06	5.72E-06	–0.903	4492.0	–10.870	2.905
HCC	-	-	-	-	-	-	-

and having differences between these values. Their corrosion potentials exceeded 100 mv, i.e. a passivity window of ΔE = Epp – Ecorr ≥ 100 mV, and an indication of tendencies to passivate [25].

4 Conclusions

From the foregoing, it can be concluded that both HCC and VCC conversion coatings outperformed uncoated Al6061 in terms of corrosion resistance and improved paint adhesion. The corrosion rates at 24 h of exposure in saline environments are, HCC, 0.024 mm/year; VCC, 0.092 mm/year and uncoated Aluminium, 0.549 mm/year. VCC and HCC are likely good replacements for chromate conversion coatings. The reducible vanadate and molybdate/vanadate ions in VCC and HCC respectively confer the term 'smart coating' on these inorganic-inorganic hybrid coatings.

References

[1] M. Oki, A. A. Adediran, P. P. Ikubanni, O. S. Adesina, A. A. Adeleke, S. A. Akintola, F. Edoziuno, and A. Aleem, "Results in engineering corrosion rates of green novel hybrid conversion coating on aluminium 6061," *Results in Engineering*, vol. 7, 2020, Art. no. 100159.

[2] *American Society for Testing and Materials*, ASTM B449-93(2015), 2015.

[3] G. Yoganandan, K. P. Premkumar, and J. N. Balaraju, "Evaluation of corrosion resistance and self-healing behavior of zirconium-cerium conversion coating developed on AA2024 alloy," *Surface and Coatings Technology*, vol. 270, pp. 249–258, 2015.

[4] I. Milošev and G. S. Frankel, "Review — conversion coatings based on zirconium and/or titanium," *Journal of the Electrochemical Society*, vol. 165, no. 3, pp. C127–C144, 2018.

[5] Z. Gao, D. Zhang, X. Li, S. Jiang, and Q. Zhang, "Current status, opportunities and challenges in chemical conversion coatings for zinc," *Colloids Surfaces A*, vol. 546, pp. 221–236, 2018.

[6] Z. Mahidashti, T. Shahrabi, and B. Ramezanzadeh, "Progress in organic coatings the role of post-treatment of an ecofriendly cerium nanostructure Conversion coating by green corrosion inhibitor on the adhesion and corrosion protection properties of the epoxy coating," *Progress in Organic Coatings*, vol. 114, pp. 19–32, 2018.

[7] J. J. Alba-Galvín, L. González-Rovira, F. J. Botana, M. Lekka, F. Andreatta, L. Fedrizzi, and M. Bethencourt, "Application of commercial surface pretreatments on the formation of cerium conversion coating (CeCC) over high-strength aluminum alloys 2024-T3 and 7075-T6," *Metals*, vol. 11, no. 6, 2021, Art. no. 930.

[8] A. E. Hughes and M. Resources, *Conversion Coatings*. Amsterdam, Netherlands: Elsevier, 2018.

[9] J. Qi, L. Gao, Y. Li, Z. Wang, G. E. Thompson, and P. Skeldon, "An optimized trivalent chromium conversion coating process for AA2024-T351 alloy for AA2024-T351 alloy," *Journal of the Electrochemical Society*, vol. 164, no. 7, pp. C390–C395, 2017.

[10] M. Oki, A. A. Adediran, B. Ogunsemi, and O. Oluwole, "Improvement in corrosion resistance of aluminium alloy by permanganate-based conversion coating," *Journal of Physical Science*, vol. 29, no. 2, pp. 13–24, 2018.

[11] C. Liang, Z. Lv, Y. Zhu, S. Xu, and H. Wang, "Applied surface science protection of aluminium foil AA8021 by molybdate-based conversion coatings," *Applied Surface Science*, vol. 288, pp. 497–502, 2014

[12] M. N. Solution, Š. Gavrilo, and I. Milo, "Electrochemical behavior and self-sealing ability of zirconium conversion coating applied on aluminum alloy 3005 in 0.5 M NaCl solution," *Journal of the Electrochemical Society*, vol. 167, no. 2, 2020, Art. no. 021509.

[13] B. Y. Shim, H. Kim, C. N. Han, Y. B. Jang, and J. W. Yun, "Characteristics of Cr (III) -based conversion coating solution to apply aluminum alloys for improving anti-corrosion properties," *Journal of the Microelectronics and Packaging Society*, vol. 23, no. 4, pp. 79–85, 2016.

[14] C. Cai, X.Q. Liu, X. Tan, G.D. Li, H. Wang, J. M. Li, and JJ. F. Li, "A Zr^{-} and Cr (III) -containing conversion coating on Al alloy 2024-T3 and its self-repairing behavior," *Materials and Corrosion*, vol. 68, no. 3, pp. 338-346, 2017

[15] J. T. Qi, T. Hashimoto, J. R. Walton, X. Zhou, P. Skeldon, and G. E. Thompson, "Trivalent chromium conversion coating formation on

aluminium," *Surface and Coatings Technology*, vol. 280, pp. 317–329, 2017

[16] J. Qi, J. Swiatowska, P. Skeldon, and P. Marcus, "Chromium valence change in trivalent chromium conversion coatings on aluminium deposited under applied potentials," *Corrosion Science*, vol. 167, 2020, Art. no. 108482.

[17] T. G. Harvey, "Cerium-based conversion coatings on aluminium alloys : A process review Cerium-based conversion coatings on aluminium alloys: A process review," *Corrosion Engineering, Science and Technology*, vol. 48, pp. 248–269, 2013.

[18] M. Oki and E. Charles, "Chromate conversion coating on Al–0.2 wt% Fe alloy," *Materials Letters*, vol. 63, no. 23, pp. 1990–1991, 2009.

[19] M. M. Kim, B. Kapun, U. Tiringer, G. Šekularac, and I. Milošev, "Protection of aluminum alloy 3003 in sodium chloride and simulated acid rain solutions by commercial conversion coatings containing Zr and Cr," *Coatings*, vol. 9, no. 9, 2019, Art. no. 563.

[20] A. Salam, I. Doench, and H. Möhwald, "Electrochimica acta assessment of a one-step intelligent self-healing vanadia protective coatings for magnesium alloys in corrosive media," *Electrochimica Acta*, vol. 56, no. 5, pp. 2493–2502, 2011.

[21] H. Guan and R. G. Buchheit, "Corrosion protection of aluminum alloy 2024-T3 by vanadate conversion coatings," *Corrosion*, vol. 60, no. 3, pp. 284–296, 2004.

[22] P. Wang, X. Dong, and D. W. Schaefer, "Structure and water-barrier properties of vanadate-based corrosion inhibitor films," *Corrosion Science*, vol. 52, no. 3, pp. 943–949, 2010.

[23] Z. Zou, N. Li, D. Li, H. Liu, and S. Mu, "A vanadium-based conversion coating as chromate replacement for electrogalvanized steel substrates," *Journal of Alloys and Compounds*, vol. 509, no. 2, pp. 503–507, 2011.

[24] Y. Ma, N. Li, D. Li, M. Zhang, and X. Huang, "Applied surface science characteristics and corrosion studies of vanadate conversion coating formed on," *Applied Surface Science*, vol. 261, pp. 59–67, 2012.

[25] G. Šekularac, J. Kovač, and I. Milošev, "Comparison of the electrochemical behaviour and self-sealing of zirconium conversion coatings applied on aluminium alloys of series 1xxx to 7xxx," *Journal of The Electrochemical Society*, vol. 167, no. 11, 2020, Art. no. 111506.